J Am Soc Nephrol 14: 2767–2774, 2003

Ureteric Bud Apoptosis and Renal Hypoplasia in Transgenic *PAX2-Bax* Fetal Mice Mimics the Renal-Coloboma Syndrome

ALISON DZIARMAGA*, PATSY CLARK†, CHERIE STAYNER‡, JEAN PIERRE JULIEN§, ELENA TORBAN¶, PAUL GOODYER*†, and MICHAEL ECCLES†‡

**Department of Human Genetics, McGill University, Montreal, Quebec, Canada; †Department of Paediatrics, Montreal Children's Hospital, McGill University, Montreal, Quebec, Canada; ‡Department of Pathology, University of Otago, Dunedin, New Zealand; §Centre for Research in Neuroscience, Montreal General Hospital, McGill University, Montreal, Quebec, Canada; and ¶Department of Biochemistry, McGill University, Quebec, Canada.*

Abstract. In humans, *PAX2* haploinsufficiency causes renal-coloboma syndrome (RCS) involving eye abnormalities, renal hypoplasia, and renal failure in early life. The authors previously showed that heterozygous mutant *Pax2* mice have smaller kidneys with fewer nephrons, associated with elevated apoptosis in the ureteric bud (UB). However, *PAX2* may have a variety of developmental functions such as effects on cell fate and differentiation. To determine whether apoptosis alone is sufficient to cause a UB branching deficit, the authors targeted a pro-apoptotic gene (*Baxα*) to the embryonic kidney under the control of human *PAX2* regulatory elements. The exogenous *PAX2* promoter directed *Baxα* gene expression specifically to the developing kidney UB, eye, and mid/hindbrain. At E15.5 *PAX2Promoter-Baxα* fetal mice exhibited renal hypoplasia, elevated UB apoptosis, and retinal defects, mimicking the phenotype observed in RCS. The kidneys of E15.5 *PAX2Promoter-Baxα* fetal mice were 55% smaller than those of wild-type fetal mice, and they contained 70% of the normal level of UB branching. The data indicate that loss of *Pax2* anti-apoptotic activity is sufficient to account for the reduced UB branching observed in RCS and suggest that elevated UB apoptosis may be a key process responsible for renal hypoplasia. The authors propose a morphogenic unit model in which cell survival influences the rate of UB branching and determines final nephron endowment.

In humans and mice, heterozygous *PAX2* mutations cause kidney, eye, and central nervous system abnormalities, constituting a syndrome called renal-coloboma syndrome (RCS) (1–3). The kidney abnormalities in patients with RCS involve primary renal hypoplasia, which together with optic nerve colobomas represent the major presenting features of RCS (3). Mutations in *PAX2* have also been identified in patients with isolated primary renal hypoplasia, including oligomeganephronia (renal hypoplasia with glomerular hypertrophy) (4,5). Analyses of renal biopsies from children with either RCS or oligomeganephronia show that renal hypoplasia is secondary to mechanisms leading to a paucity of nephrons (3–5). This observation points to a deficit in ureteric bud (UB) branching in patients carrying *PAX2* mutations, as UB branching is a prerequisite for nephron formation. Although *PAX2* mutations lead to renal hypoplasia, the mechanism by which reduced *PAX2* dosage leads to a decreased extent of UB branching and lack of nephrons in patients with RCS is not clear.

Mammalian kidney development begins early in embryonic life, when the UB emerges from the nephric duct. UB growth is elicited by trophic signals (*e.g.*, glial cell–derived neurotrophic factor [GDNF] and Wnt2b) from the adjacent mesenchyme, which activate specific receptors on the UB cell surface (6,7). As the UB penetrates the mesenchyme, it begins to arborize, inducing individual nephrons at the tip of each of its branches as it grows. Signals from each branch tip recruit adjacent mesenchymal cells to condense at its lateral aspect and undergo rapid phenotypic transformation into polarized epithelial cells of the nephron. Each emerging nephron fuses with the UB, allowing egress of filtered fluid. The extent of UB arborization, which has been achieved by the time nephrogenesis ends in the perinatal period, determines the final number of nephrons constituting the individual's nephron endowment for life.

This complex process is orchestrated by key developmental transcription factors. Among the earliest of these is *PAX2*, which is expressed in the nephric duct and uninduced mesenchyme before formation of the metanephros, throughout the arborizing UB and finally in the condensing mesenchyme after induction (8). With completion of nephrogenesis, expression of the renal *PAX2* gene is rapidly downregulated. In 1996, a strain of mice ($Pax2^{1Neu}$) was identified with RCS due to a sponta-

Received October 11, 2002. Accepted August 7, 2003.
Paul Goodyer and Michael Eccles contributed equally to this work.
Correspondence to Dr. Michael Eccles, Department of Pathology, University of Otago, Dunedin 9015, New Zealand. Phone: +64-3479-7878; Fax: +64-3479 7139; E-mail: meccles@otago.ac.nz

1046-6673/1411-2767
Journal of the American Society of Nephrology

DOI: 10.1097/01.ASN.0000094082.11026.EE

neous *Pax2* mutation identical to the most common mutation in humans with RCS (9). In fetal ($Pax2^{1Neu\ +/-}$) mutant mice, we showed that the renal hypoplasia is associated with reduced nephron number and elevated apoptosis in the UB epithelium (3,10). Furthermore, a direct role for *Pax2* in survival of UB cells is supported by our observation that mIMCD-3 collecting duct cells undergo apoptosis when transfected with an antisense *Pax2* expression construct (10). In contrast, *Pax2* null mutant mice have bilateral renal agenesis; although the caudal portion of the nephric duct initially forms, it then degenerates (9,11).

Although mutations in *Pax2* are associated with elevated levels of UB apoptosis, it is not known whether apoptosis alone accounts for suboptimal UB arborization in RCS. Indeed, relatively high basal levels of apoptosis are known to occur during development of the fetal kidney and other organs, but the significance of this apoptosis is not understood (12,13). Normally, *Pax2* is expressed in cells of the mesenchymal lineage as well as in the ureteric bud, yet we observed no significant increase in mesenchymal cell apoptosis in *Pax2* mutant mice (3). *Pax2* activates GDNF in metanephric mesenchyme (14), and we found effects of *Pax2* on E-cadherin expression (15). Arguably, therefore, *Pax2* haploinsufficiency disturbs key steps in cell differentiation, and the apoptosis in ($Pax2^{1Neu\ +/-}$) mutant mice is the consequence of cells not achieving their developmental fate. It is, however, important to know whether apoptosis occurring in the UB is sufficient to directly cause renal hypoplasia or whether additional mesenchyme-related functional deficits are also required. Our hypothesis is that the enhanced susceptibility of UB cells to programmed cell death in *Pax2* haploinsufficiency directly compromises the rate of UB arborization and has a direct role in causing renal hypoplasia.

To examine the latter hypothesis, we have targeted an apoptosis-inducing transgene to the developing UB of fetal kidneys. We show that transgenic fetal mice expressing the proapoptotic *PAX2Promoter-Baxα* transgene in embryonic kidney, eye, and brain under the control of exogenous *PAX2* regulatory elements have elevated UB apoptosis and renal hypoplasia due to reduced UB branching. These data demonstrate that enhanced UB cell apoptosis during renal development compromises UB arborization, mimicking the RCS phenotype caused by *PAX2* mutations. We propose the existence of an elemental UB morphogenic unit with an intrinsic mechanism for timing iterative branching events. In this model, susceptibility of the UB to apoptosis regulates UB arborization during kidney development.

Materials and Methods

PAX2Promoter-Baxα Transgene Construction

An *IRES-lacZ* vector, generously provided by Dr. Daniel Dufort (McGill University, Montreal), was modified by removing one *Spe*I restriction site and inserting an oligonucleotide containing five unique restriction sites to facilitate cloning. A 4-kb *Acc*I/*Not*I fragment containing 5' flanking sequences of the human *PAX2* gene (16) was ligated into compatible *Nar*I and *Not*I sites in the modified *IRES*/*lacZ* vector. A *Not*I/*Eco*RV fragment of *Baxα* cDNA was then ligated downstream from the promoter, using *Not*I and an end-filled *Spe*I site in the *IRES* vector. The GenBank accession number for the 4.2-kb *Apa*I/*Nco*I fragment of the human *PAX2* promoter and flanking sequences is AF515729.

Transient Transfections and Cell Culture

The activity and tissue specificity of a 4.2-kb upstream region of the *PAX2* gene was analyzed in transient transfections of mIMCD-3, HEK293, COS-7, and NIH 3T3 cell lines. Plasmid DNA preparation, cell culture, and transient transfections using FuGene 6 (Roche) were carried out as described (16), with modifications. Briefly, cells at 50 to 70% confluency were co-transfected with 0.4 μg of pRSV-β-gal and 0.8 μg of human *PAX2Promoter*-pGL2Basic. Cells were harvested 48 h after transfection, lysed in a passive lysis buffer (Promega), and assayed for firefly luciferase and β-gal (Galacto-Star, TROPIX). Transfections were performed in replicates of six on three separate occasions.

Generation of Transgenic Mice

*Xho*I linearized plasmid DNA from the *PAX2Promoter-Baxα* construct was diluted to 2 ng/μl and microinjected into the male pronuclei of C57B/6J X C3H fertilized eggs. Injected eggs were then transferred into the oviducts of pseudopregnant females. Transgenic fetal mice were identified by PCR amplification of the *IRES* region from DNA obtained from tails (animals which came to term) or hind limb (embryos). Transgenic mice were viable and fertile. PCR primers used for genotyping transgenic mice were, *Bax*3'F: 5'-TAATCTTGAAGTCTCCATCCG-3', and IRES3'R: 5'-CAGATCAGATCCCATACAATG-3', which amplified a 500-bp fragment from the *PAX2Promoter-Baxα* construct.

β-Galactosidase Detection

Fetal age was determined by timed pregnancy and morphologic analysis according to Kaufman's Atlas of Mouse Development. Whole-mount histochemistry for β-galactosidase was carried out as described (17); embryos were stained overnight. After whole-mount staining, embryos were washed and fixed in 4% paraformaldehyde, dehydrated in ethanol, embedded in paraffin wax, and sectioned at 7 μm.

Maximal Kidney Cross-Sectional Area Determination, Glomerular Counting, and TUNEL Staining to Determine the Number of Cells Undergoing Apoptosis

The cross-sectional area was determined in kidney sections showing the maximal cross-sectional area in comparison to adjacent sections. To do this, whole embryos were paraffin-embedded in the same orientation before sagittal serial sectioning. Sections were stained with nuclear red, and the section containing the maximal cross-sectional area was measured for each kidney ($n = 9$ wild-type kidneys; $n = 10$ *Bax* transgenic kidneys). Photographs of each section showing the maximal cross-sectional area were taken at 4×.

For determination of the number of glomeruli in wild-type and *Bax* transgenic kidneys, the glomeruli, S-shaped bodies, and comma-shaped bodies were counted in sections with the maximal cross-sectional area ($n = 8$ kidneys from 5 wild-type fetal mice; and $n = 10$ kidneys from 6 *Bax* transgenic fetal mice). The sections used for the glomerular counts were the same sections as those used to determine the maximal cross-sectional area above. In addition, glomeruli were counted with the same methodology in one kidney each from two

additional *PAX2Promoter-Bax* transgenic animals, yielding counts of 13 and 13 glomeruli, respectively.

For determination of the number of cells undergoing apoptosis in wild-type and *Bax* transgenic kidneys, terminal deoxynucleotidyl-transferase (TdT)-mediated dUTP nick-end labeling (TUNEL) staining was performed as described (3). The number of cells that stained positive for TUNEL in the UB, which was observed to contain the majority of TUNEL-positive staining, were counted. Two sections from each kidney, near to the center of the kidney, were used for counting ($n = 5$ kidneys from 4 wild-type fetal mice; $n = 5$ kidneys from 4 *Bax* transgenic fetal mice). In two of the *PAX2Promoter-Bax* transgenic fetal mice, there was only one kidney present. The area in mm^2 occupied by the UB in the sections was measured, and the data were expressed as a ratio of TUNEL-positive apoptotic cells/mm^2.

Bax Immunostaining and Western Blot

Embryonic 7-μm mouse sections were deparaffinized, rehydrated, and boiled twice for 5 min in 10 mM citrate buffer. Endogenous peroxidase activity was quenched using 3% H_20_2 (in methanol) for 15 min at room temperature. After 30-min incubation with blocking serum, sections were incubated with primary, polyclonal rabbit anti-Bax antibody (Santa Cruz Biotechnology) at 4°C overnight, followed by staining using a Vectastain ABC universal kit (Vector Laboratories) as described by the manufacturer, and incubation with DAB (3). Sections were counterstained in 0.5% methyl green for 1 min each, dehydrated, and mounted with Permount.

Western blot analysis to detect Bax protein was carried out using a polyclonal rabbit anti-Bax antibody (Santa Cruz Biotechnology), followed by detection with a peroxidase goat anti-rabbit IgG (Perkin Elmer). To detect actin in Western blots, a monoclonal mouse anti-actin antibody (Oncogene) was used, followed by detection with a peroxidase goat anti-mouse IgM (Calbiochem). The secondary antibody-peroxidase conjugate was detected using chemiluminescence as described by the manufacturer (Calbiochem).

Dolichos Biflorus Agglutinin (DBA) Staining

For counting of UB branch tips, E15.5 kidneys were microdissected from transgenic fetal mice. Each kidney was fixed in 200 μl of 4% formaldehyde in phosphate-buffered saline (PBS) for 48 h. The fixative was removed, and the kidneys were washed 4 $\times$ 10 min at room temperature in 500 μl of PBS-T (PBS + 1% Triton X-100). After washing, kidneys were incubated in 200 μl of Dolichos Biflorus Agglutinin-FITC (DBA-FITC) in PBS (1:100 dilution) overnight at 4°C, as described (18). The DBA-FITC was removed, and kidneys were washed for 10 min at room temperature in 500 μl of PBS-T. Kidneys were then incubated at 4°C overnight in PBS-T or until ready to photograph. For photographing, whole kidneys were placed on a slide under a cover slip with no mounting solution. Images were obtained, and the total number of UB terminal ends per kidney was counted directly on the computer screen.

Results

Generation of PAX2Promoter-Bax Transgenic Fetal Mice

A 4-kb DNA fragment containing the human *PAX2* promoter (16) was cloned into a promoterless expression vector containing murine *Bax*α cDNA and used to generate *PAX2Promoter-Bax* transgenic mice. This expression construct also carried a *lacZ* reporter gene flanked by a 5' internal ribosome entry site (*IRES*) sequence, allowing independent translation of β-galactosidase under the transcriptional control of the *PAX2* promoter (Figure 1A). In cell culture transfection experiments, the 4.2-kb h*PAX2* promoter was able to drive high levels of reporter gene expression in specific kidney epithelial cell lines, particularly murine inner medullary collecting duct cells (mIMCD-3) (Figure 1B). High conservation of sequence identity between the human *PAX2* promoter and the murine *Pax2* promoter was observed between 3290 and 4158 (19) and also in a 400-bp region, which contained 89% identity between positions 383 and 782 (Figure 1A). In mice, the 400-bp sequence had previously been shown to direct expression of *Pax2* in the Wolffian duct, UB, and collecting ducts during development (17). Transgenic mice were generated by pronuclear injection and germline integration of the *PAX2Promoter-Bax* construct (Figure 1C). Eleven *PAX2Promoter-Bax* transgenic embryos were analyzed at E13.5 or E15.5. In addition, six founder *PAX2Promoter-Bax* transgenic mice were born. No significant skewing of Mendelian ratios was observed in 45 offspring from three of these founders, suggesting that there is little or no embryonic lethality as a result of the presence of the transgene.

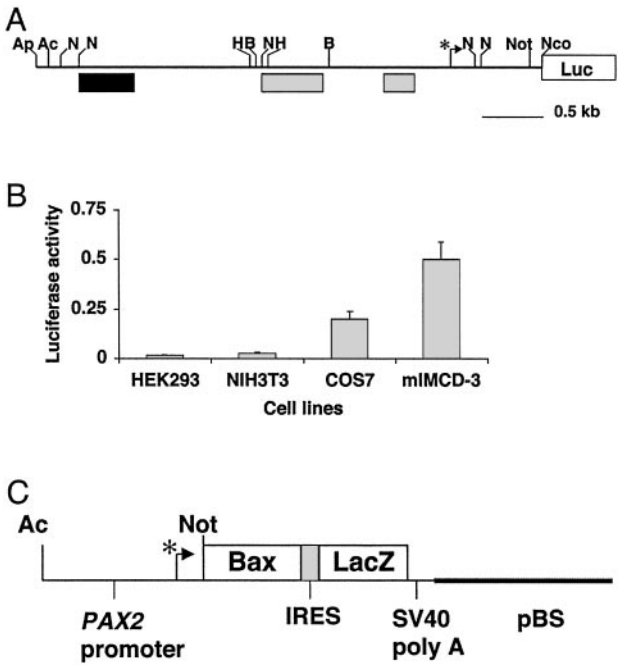

Figure 1. Construction of the *PAX2Promoter-Bax*α transgene. (A) A 4.2-kb *Apa*I/*Nco*I fragment containing the human *PAX2* promoter and flanking regulatory sequences was cloned into the vector pGL2basic (Luc). A 0.4-kb region of 89% identity with the murine *Pax2* promoter sequence was identified near the 5' end of the human *PAX2* sequence (black box), upstream from the transcription start site (asterisk). (B) Transfection of the *PAX2Promoter-Luc* construct into four different cell lines revealed high activity of the *PAX2* promoter, with highest expression observed in inner medullary collecting duct cells (mIMCD-3) kidney collecting duct cells. (C) A 4-kb *Acc*I/*Not*I fragment of the *PAX2* promoter was inserted into an *IRES*/*lacZ* expression vector, containing murine *Bax*α (Bax) and *IRES-lacZ* (LacZ) genes. IRES, internal ribosome entry site; pBS, pbluescript; Ac, *Acc*I; Ap, *Apa*I; B, *Bam*HI; H, *Hin*dIII, N, *Nar*I, Nco, *Nco*I, Not, *Not*I.

Expression of β-Galactosidase Reporter and Baxα during Kidney Development in PAX2Promoter-Bax Transgenic Mice

The murine *Pax2* gene is expressed in the developing midbrain and hindbrain, eye, ear, and fetal urogenital tract, including Wolffian and Mullerian ducts, UB, collecting ducts, and condensing mesenchyme of fetal kidney (8,20). To determine whether the *PAX2Promoter-Bax* transgene was expressed in the correct *Pax2*-specific pattern, we analyzed expression of the *lacZ* reporter gene in transgenic embryos. Strong β-galactosidase staining was identified in the kidneys and mid/hindbrain of wholemount E15.5 embryos (Figure 2A). A more detailed analysis of tissue-specificity and temporal regulation of the transgene showed that the transgene was expressed in the developing urogenital tract, including Wolffian duct, UB, and collecting ducts, and in the developing eye of E15.5 embryos (Figure 2, B through D). High levels of expression of the transgene were observed in the fetal hindbrain, eyes, and collecting ducts, mimicking the pattern of strongest endogenous *Pax2* expression (8,20).

The transgenic expression pattern (UB and collecting duct) was confirmed by immunohistochemical staining of E15.5 transgenic and wild-type fetal mice with an anti-Bax antibody. Elevated *Baxα* expression was detected in the UB and collecting ducts of E15.5 transgenic fetal mice (Figure 2F). Endogenous *Baxα* expression was present in the UB and collecting ducts in E15.5 wild-type kidneys but was at a lower level in wild-type kidneys than in the *PAX2Promoter-Bax* transgenic fetal mice, as shown by immunohistochemistry (Figure 2G). When mIMCD-3 cells transfected with the *PAX2Promoter-Bax* transgene were analyzed by Western blot using the anti-Bax antibody, there was a greater level of Bax expression in the transfected cells than in nontransfected cells (Figure 3), again suggesting that the *Bax* transgene was relatively strongly expressed under the control of the *PAX2* promoter.

Apoptosis in PAX2Promoter-Bax Transgenic Kidneys

As there were high levels of expression of the pro-apoptotic *Baxα* gene in the UB of *PAX2Promoter-Bax* transgenic fetal mice, we analyzed the pattern and number of cells undergoing apoptosis in the fetal kidneys of transgenic and wild-type mice. In transgenic E15.5 kidneys, high levels of apoptosis were evident in UB and collecting duct epithelium, whereas apoptosis levels in the UB and collecting ducts of wild-type fetal mice were very low (Figure 4, A and B). The number of apoptotic cells per mm^2 in the transgenic fetal kidney ureteric bud epithelia was more than tenfold higher than that in wild-type kidneys (Figure 4C). By eye, apoptosis levels did not appear to be elevated in other regions of the kidneys of *PAX2Promoter-Bax* transgenic fetal mice, including in the condensing mesenchyme or glomeruli.

Histologic Analyses of Kidney Formation in PAX2Promoter-Bax Transgenic Fetal Mice

The kidneys of E15.5 transgenic fetal mice ($n = 10$) were 55% (± 4% SEM) smaller in maximal cross-sectional area than those of wild-type fetal mice ($n = 9$) (Figure 5). The

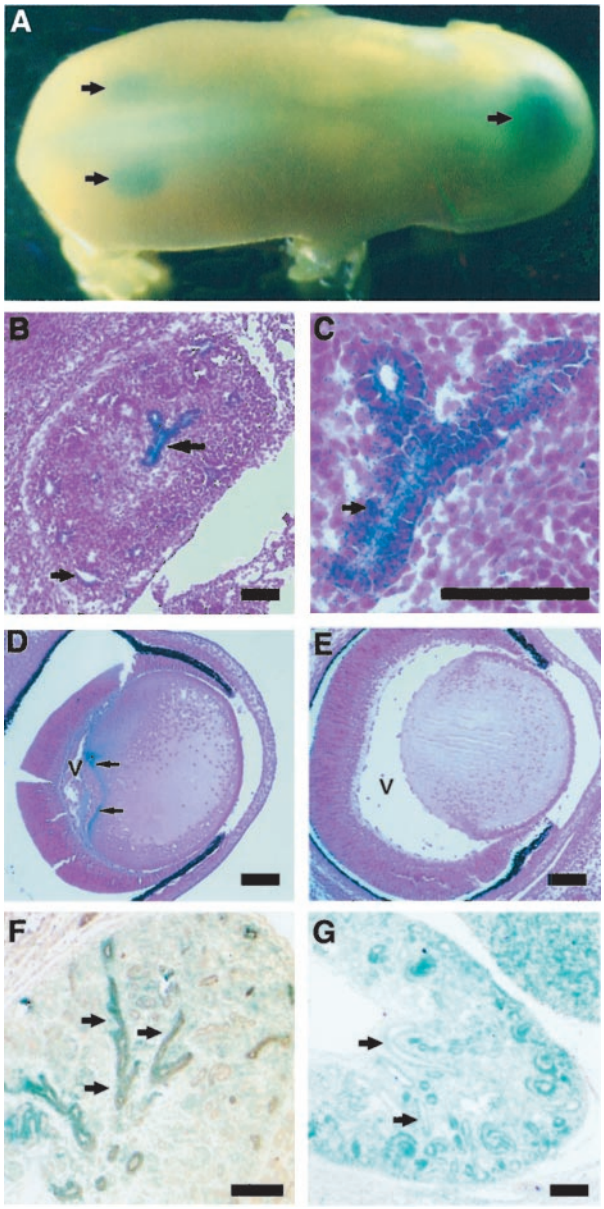

Figure 2. Expression of the *PAX2Promoter-Baxα* transgene in fetal mice. (A) Dorsal view of an E15.5 *PAX2Promoter-Baxα* wholemount transgenic mouse embryo with expression of β-galactosidase in the mid/hindbrain and kidneys (arrows). (B) Kidney section from an E13.5 *PAX2Promoter-Baxα* transgenic mouse showing expression of β-galactosidase in the collecting ducts and ureteric bud (UB; arrows). (C) Higher magnification of β-galactosidase expression in the collecting duct epithelia of an E13.5 *PAX2Promoter-Baxα* transgenic mouse. (D and E) Sagittal sections of the eye of E15.5 *Pax2Promoter-Bax* transgenic (D) and wild-type (E) fetal mice showing expression of β-galactosidase in cells lining the posterior lens and inner layer of the optic cup of the *Bax* transgenic mouse (arrows). The development of the *Pax2Promoter-Bax* transgenic mouse eye is more immature than that of the wild-type, with the inner layer of the optic cup still attached to the posterior lens cells and poor development of the vitreous body (V). (F) Kidney section of an E15.5 *PAX2Promoter-Baxα* transgenic mouse showing Baxα expression in the collecting ducts and UB (arrow), but not in condensing mesenchyme. (G) Baxα was expressed at low levels in the collecting ducts and UBs of E15.5 wild-type fetal mice. Scale bar, 100 μm.

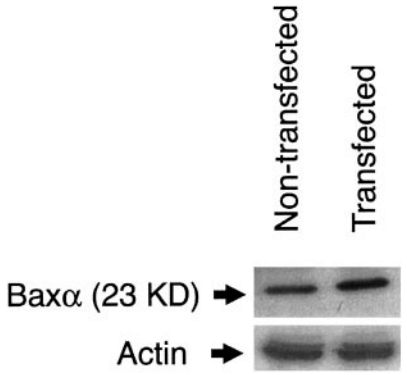

Figure 3. Western blot analysis of Baxα expression in mIMCD-3 cells transfected with the *PAX2Promoter-Baxα* construct. Protein lysates from mIMCD-3 cells that were either nontransfected or transfected with the *PAX2Promoter-Baxα* construct were analyzed by Western blot using a Bax antibody. A 23-kD Bax protein was observed in both nontransfected and *PAX2Promoter-Baxα*–transfected cells, but the band observed in *PAX2Promoter-Baxα*–transfected cells was stronger than in the nontransfected cells, indicating higher Bax expression in the transfected cells. Western blots with an anti-actin antibody were used as a control for protein loading.

reduction in kidney size was accompanied by the presence of fewer epithelial structures, including fewer glomeruli in sections of the *PAX2Promoter-Bax* transgenic kidneys compared with wild-type kidneys (Figure 6, A and B, arrows). Except for this, the glomeruli and UB in the *Bax* transgenic kidneys were approximately the same size as in wild-type fetal mice, albeit not as well developed (Figure 6, C and D). Quantifying the number of glomeruli present in the kidney sections showed that there were significantly fewer glomeruli in all sections from *PAX2Promoter-Bax* transgenic fetal mice compared with wild-type fetal mice (Figure 6E). However, despite the smaller kidney size in the *PAX2Promoter-Bax* transgenic animals, body lengths measured from crown to rump in whole fetal sections on slides, which were from the same identical sections in which the maximal cross-sectional kidney areas were determined, were not significantly different in transgenic and wild-type animals. Five wild-type animals had an average crown-rump body length of 1.27 ± 0.14 mm, whereas 11 *PAX2Promoter-Bax* transgenic animals had an average crown-rump body length of 1.20 ± 0.13 mm. The overall appearance of the wild-type and transgenic fetal sections on the slides was indistinguishable.

The reduction in the number of glomeruli in the *Bax* transgenic kidneys was confirmed by observing a reduction in the extent of UB branching in dolichos bifluoros agglutinin (DBA)-stained *PAX2Promoter-Bax* E15.5 fetal kidneys compared with wild-type kidneys (Figure 7, A through D). These results show that there were 30% (± 4% SEM) fewer UB branch tips in the *Bax* transgenic kidneys ($n = 7$) compared with wild-type kidneys ($n = 8$) (Figure 7E). Overall, the renal hypoplasia and reduction in UB branching observed in *Pax2Promoter-Bax* transgenic fetal mice was remarkably similar to that observed in kidneys from ($Pax2^{1Neu}$) heterozygous mutant mice (3).

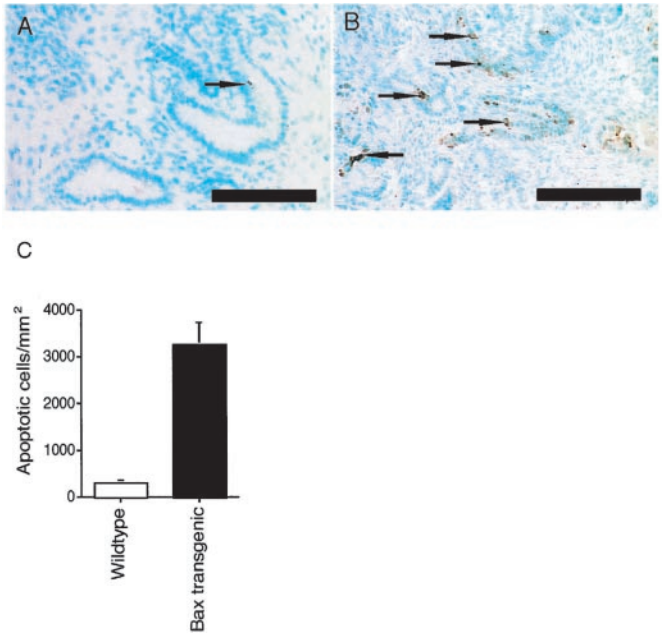

Figure 4. Apoptosis in wild-type and *PAX2Promoter-Bax* fetal kidneys. (A and B) Apoptosis, detected in kidney sections by TUNEL staining (arrows), was greatly enhanced in the UB and collecting ducts of E15.5 *PAX2Promoter-Baxα* transgenic fetal mice (B), compared with wild-type kidneys of the same age (A). Scale bar, 100 μm. (C) Quantitation of the number of cells undergoing apoptosis in *Bax* transgenic and wild-type kidneys revealed that there was significantly more apoptosis in the UB of the *PAX2Promoter-Bax* transgenic kidneys than in the wild-type kidneys, $P < 0.0001$.

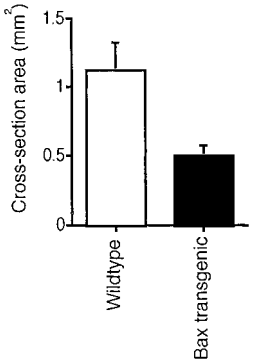

Figure 5. Kidneys from *PAX2Promoter-Baxα* transgenic fetal mice were smaller than those from wild-type fetal mice. The maximal cross-sectional area (mm^2) of E15.5 *PAX2Promoter-Baxα* transgenic kidneys was 45% of that in wild-type fetal mice, $P < 0.0001$ (SEM).

Discussion

The RCS is a rare multisystem developmental disorder, presenting with optic nerve colobomas and renal abnormalities, caused by *PAX2* mutations (1,2). Renal hypoplasia (reduced nephron number), leading to renal failure in approximately 70% of RCS patients is an important feature of this disease (1–3). During kidney development, rapid growth and iterative branching of the ureteric tree determines the number of

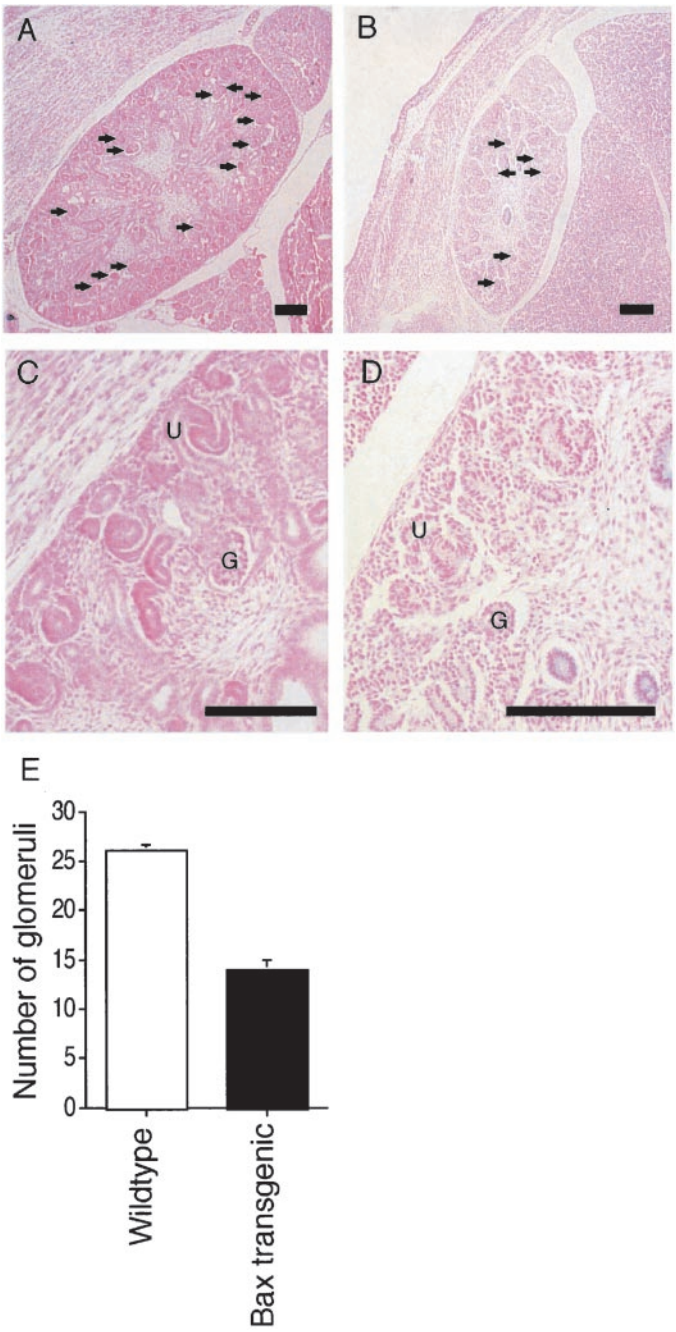

Figure 6. Reduction in the number of glomeruli and terminal UB branch ends in the kidneys of *PAX2Promoter-Baxα* transgenic fetal mice compared with wild-type fetal mice. (A and B) Tissue sections from wild-type kidneys (A) and *PAX2Promoter-Baxα* transgenic kidneys stained with nuclear red (B) showed differences in kidney size and glomerular number, with reduced numbers of glomeruli being present in the transgenic kidneys (arrows). (C and D) Tissue sections of wild-type (C) and *PAX2Promoter-Baxα* transgenic (D) kidneys at higher magnification showed that the glomeruli (G) and ureteric buds (U) were approximately similar in size and shape but that there were fewer such structures in the *PAX2Promoter-Baxα* transgenic than in the wild-type kidneys. Scale bar, 100 μm. (E) There were significantly fewer glomeruli in *PAX2Promoter-Baxα* transgenic kidneys ($n = 10$) than in wild-type kidneys ($n = 8$); $P < 0.0001$.

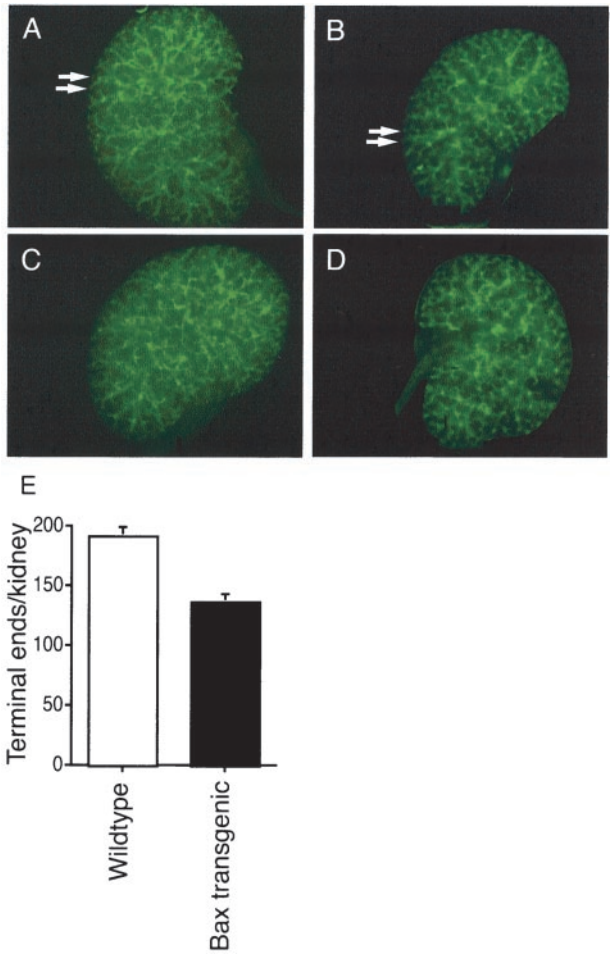

Figure 7. The number of UB terminal ends in E15.5 *PAX2Promoter-Baxα* transgenic kidneys is reduced. Fetal E15.5 kidneys were stained with DBA to assess branching morphogenesis. (A and C) Terminal ends in wild-type DBA-stained kidneys (arrows); (B and D) terminal ends in *PAX2Promoter-Bax* transgenic DBA stained kidneys (arrows). Note that the wild-type kidneys are slightly bigger and have more branches compared with the transgenic kidneys. (E) The number of UB branch terminal ends in E15.5 *PAX2Promoter-Baxα* transgenic kidneys as detected by DBA staining was 70% of that in wild-type fetal mice, $P < 0.0001$ (SEM).

nephrons formed, which constitute final nephron endowment for life. The UB cell lineage is highly protected from programmed cell death, whereas apoptosis is widespread in the metanephric mesenchyme, where it is part of normal morphogenesis (3,12,13). This study demonstrates the effect of elevated levels of UB apoptosis on kidney development and shows that elevated UB apoptosis alone is sufficient to compromise the rate of new nephron formation and mimic the RCS phenotype.

Excessive levels of randomly occurring programmed cell death in fetal kidney cells might lead to small kidneys, but not necessarily to reduced nephron number. However, our studies show that apoptosis targeted to *Pax2*-expressing cells caused small kidneys with a reduced number of UB branches. We propose the existence of a UB "morphogenic unit," which is

affected by *PAX2* mutations in RCS as illustrated by our model of UB branching morphogenesis. In this model, each UB branching event is accompanied by local interactions with mesenchyme, suppressing further UB branching (Figure 8). As each new branch lengthens, the specialized UB tips grow beyond a putative zone where UB branching is inhibited, allowing the next cycle of branching to occur. In this model, stochastic depletion of cells during extension of the UB branch would slow its linear growth rate, delaying escape from the inhibitory zone and delaying the next round of branching. Assuming that there is a finite temporal window for UB branching during renal organogenesis, the balance of survival and pro-apoptotic signals would act as a timing mechanism for the rate of UB arborization during fetal life and ultimately determine final nephron number (Figure 8).

Many factors are involved in UB branching morphogenesis, including growth-signaling pathways (21). For example, the *GDNF* gene encodes a ligand for the RET receptor expressed on the surface of UB cells; both *GDNF* and *RET* are required for UB branching, growth, and cell survival (22–24), and heterozygous *GDNF* mutations are associated with renal hypoplasia (25). The collective influence of these genes on apoptosis levels would be expected to directly affect UB branching morphogenesis and nephron number. Therefore, differences between individuals in the basal level of UB apoptosis during development might help to explain why the complement of human nephrons varies from 300,000 to 1,100,000 in the general population, although there may also be other factors that contribute to this variation (reviewed in reference 26).

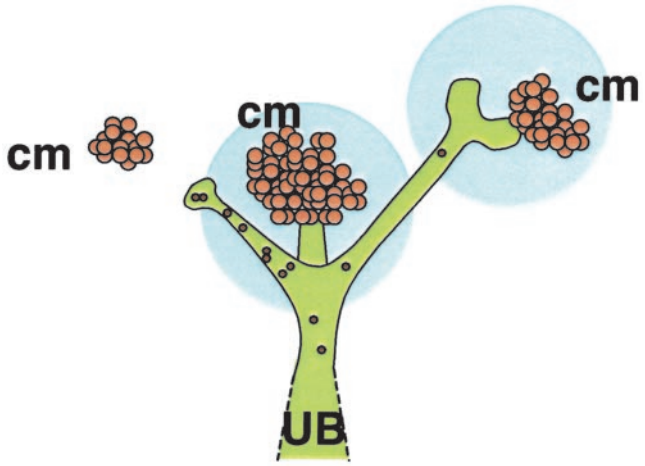

Figure 8. Proposed morphogenic unit model of UB branching morphogenesis. The UB (green) is shown with three branches. Each UB branching event is accompanied by local interactions with condensing mesenchyme (cm, shown as orange spheres), as depicted by the middle branch, which inhibits further branching in the region encompassed by the zone of inhibition (delineated by a light blue circle). Contact with the mesenchyme is postulated to inhibit branching by a diffusible factor from the mesenchyme or by signals that remain intrinsically in the UB cells for a finite number of cell divisions following contact with the mesenchyme. As each new branch lengthens, the specialized UB tips grow beyond the putative inhibitory zone (right branch), allowing the next cycle of branching to occur. Stochastic depletion of cells by apoptosis (small brown circles) during extension of the UB branch (shown in left branch) would slow its linear growth rate, delaying escape from the local inhibitory zone and delaying the next round of branching.

Further support for the morphogenic unit model arises from our observation that, in contrast to the effects of excessive apoptosis on nephron number, inhibition of apoptosis in wild-type and ($Pax2^{1Neu\ +/-}$) mutant fetal kidneys leads to increased UB branching and increased nephron number. *Ex vivo* treatment of either wild-type or ($Pax2^{1Neu\ +/-}$) mutant fetal kidneys for 2 d with the caspase inhibitor Z-VAD-fmk, increased UB branching in DBA-stained kidney explants compared with untreated explants (Clark *et al.*, unpublished observation). Taken together, these results suggest that the hypoplastic renal phenotype in RCS is determined primarily by loss of *Pax2* anti-apoptotic function in UB cells.

As well as its role in kidney development, *Pax2*-mediated cell survival may also be important for the development of other organs, including the eye. Expression of the *PAX2Promoter-Baxα* transgene in embryonic retina was associated with an immature stage of eye development, with attachment of the inner layer of the optic cup to the posterior lens cells, and poor development of the vitreous body (Figure 2, D and E). These data suggest that there may be a role for *Pax2*-mediated cell survival in eye development.

In conclusion, we have examined the role of apoptosis in organ patterning by targeting *Baxα* expression to specific cell lineages during development. The studies presented here illuminate a functional relationship between apoptosis, patterning in the UB, and branching morphogenesis, whereby increased susceptibility to apoptosis in the UB lineage during fetal kidney development is sufficient to recapitulate the nephron deficit of RCS. Our results predict that potential therapies, involving inhibition of apoptosis during development may be used to treat RCS, or primary renal hypoplasia, if detected *in utero*. Consequently, nephron rescue therapies, if directed to the developing kidney, might fully restore the normal nephron complement in affected patients.

Acknowledgments

The authors thank Dr. Daniel Dufort for the *IRES-LacZ* expression vector, Dr. Gordon Shore for *Bax* cDNA and anti-Bax antibody, and Dr. Cynthia Goodyer and Dr. Fernanda Da Silva-Tatley for advice on cloning and discussions. Funding for this work was from the Canadian CIHR, the Cancer Society and the Health Research Council of New Zealand. ME was supported by a James Cook Fellowship of the Royal Society of New Zealand.

References

1. Eccles MR, Schimmenti LA: Renal-coloboma syndrome: a multi-system developmental disorder caused by *PAX2* mutations. *Clin Genet* 56: 1–9, 1999
2. Sanyanusin P, Schimmenti LA, McNoe LA, Ward TA, Pierpont MEM, Sullivan MJ, Dobyns WB, Eccles MR: Mutation of the *PAX2* gene in a family with optic nerve colobomas, renal anomalies and vesicoureteral reflux. *Nature Genet* 9: 358–364, 1995
3. Porteous S, Torban E, Cho NP, Cunliffe H, Chua L, McNoe L, Ward T, Souza C, Gus P, Giugliani R, Sato T, Yun K, Favor J,

Sicotte M, Goodyer P, Eccles M: Primary renal hypoplasia in humans and mice with *PAX2* mutations: evidence of increased apoptosis in fetal kidneys of *Pax2*^{1Neu} +/− mutant mice. *Hum Mol Genet* 9: 1–11, 2000
4. Salomon R, Tellier AL, Atie-Bitach T, Amiel J, Vekemans M, Lyonnet S, Dureau P, Niaudet P, Gubler MC, Broyer M: *PAX2* mutations in oligomeganephronia. *Kidney Int* 59: 457–462, 2001
5. Nishimoto K, Iijima K, Shirakawa T, Kitagawa K, Satomura K, Nakamura H, Yoshikawa N (2001): *PAX2* gene mutation in a family with isolated renal hypoplasia. *J Am Soc Nephrol* 12: 1769–1772, 2001
6. Bard JBL: Growth and death in the developing mammalian kidney: signals, receptors and conversations. *BioEssays* 24: 72–82, 2002
7. Davies JA, Davey MG: Collecting duct morphogenesis. *Pediatr Nephrol* 13: 535–541, 1999
8. Dressler GR, Deutsch U, Chowdhury K, Nornes HO, Gruss P: *Pax2*, a new murine paired-box-containing gene and its expression in the developing excretory system. *Development* 109: 787–795, 1990
9. Favor J, Sandulache R, Neuhauser-Klaus A, Pretsch W, Chatterjee B, Senft E, Wurst W, Blanquet V, Grimes P, Sporle R, Schughart K: The mouse *Pax2*^{1Neu} mutation is identical to a human *PAX2* mutation in a family with renal-coloboma syndrome and results in developmental defects of the brain, ear, eye, and kidney. *Proc Natl Acad Sci USA* 93: 13870–13875, 1996
10. Torban E, Eccles MR, Favor J, Goodyer PR: *PAX2* suppresses apoptosis in renal collecting duct cells. *Am J Pathol* 157: 833–842, 2000
11. Torres M, Gomez-Pardo E, Dressler G, Gruss P: Pax-2 controls multiple steps of urogenital development. *Development* 121: 4057–4065, 1995
12. Koseki C, Herzlinger D, al Awqati Q: Apoptosis in metanephric development. *J Cell Biol* 119: 1327–1333, 1992
13. Coles HS, Burne J, Raff MC: Large-scale normal cell death in the developing rat kidney and its reduction by epidermal growth factor. *Development* 118: 777–784, 1993
14. Brophy PD, Ostrom L, Lang KM, Dressler GR: Regulation of ureteric bud outgrowth by *Pax2*-dependent activation of the glial derived neurotrophic factor gene. *Development* 128: 4747–4756, 2001
15. Torban E, Goodyer PR: Effects of *PAX2* expression in a human fetal kidney (HEK293) cell line. *Biochim Biophys Acta* 1401: 53–62, 1998
16. Stayner CK, Cunliffe HE, Ward TA, Eccles MR: Cloning and characterization of the human *PAX2* promoter. *J Biol Chem* 273: 25472–25479, 1998
17. Kuschert S, Rowitch DH, Haenig B, McMahon AP, Kispert A: Characterization of Pax-2 regulatory sequences that direct transgene expression in the Wolffian duct and its derivatives. *Dev Biol* 229: 128–140, 2001
18. Igarashi P, Shashikant CS, Thomson RB, Whyte DA, Liu-Chen S, Ruddle FH, Aaronson PS: Ksp-cadherin gene promoter. II. Kidney-specific activity in transgenic mice. *Am J Physiol* 277: F599–F610, 1999
19. Ryan G, Steele-Perkins V, Morris JF, Rauscher FJIII, Dressler GR: Repression of *Pax-2* by *WT1* during normal kidney development. *Development* 121: 867–875, 1995
20. Nornes HO, Dressler GR, Knapik EW, Deutsch U, Gruss P: Spatially and temporally restricted expression of *Pax2* during murine neurogenesis. *Development* 109: 797–809, 1990
21. Fisher CE, Michael L, Barnett MW, Davies JA: Erk MAP kinase regulates branching morphogenesis in the developing mouse kidney. *Development* 128: 4329–4338, 2001
22. Towers PR, Woolf AS, Hardman P: Glial cell line-derived neurotrophic factor stimulates ureteric bud outgrowth and enhances survival of ureteric bud cells *in vitro*. *Exp Nephrol* 6: 337–351, 1998
23. Pepicelli CV, Kispert A, Rowitch DH, McMahon AP: GDNF induces branching and increased cell proliferation in the ureter of the mouse. *Dev Biol* 192: 193–198, 1997
24. O'Rourke DA, Sakurai H, Spokes K, Kjelsberg C, Takahashi M, Nigam S, Cantley L: Expression of c-ret promotes morphogenesis and cell survival in mIMCD-3 cells. *Am J Physiol* 276: F581–F588, 1999
25. Cullen-McEwen LA, Drago J, Bertram JF: Nephron endowment in glial cell line-derived neurotrophic factor (GDNF) heterozygous mice. *Kidney Int* 60: 31–36, 2001
26. Clark AT, Bertram JF: Molecular regulation of nephron endowment. *Am J Physiol* 276: F485–F497, 1999